

## **Deposition of Anti-Corrosion Coatings by Atmospheric Pressure Plasma Jet**

**J. S. C. Wills, D. A. Guzonas and A. Chiu**

Atomic Energy of Canada Limited, Chalk River, Ontario, Canada

### **Abstract**

An atmospheric-pressure, non-equilibrium plasma jet is currently under investigation at Chalk River Laboratories for the application of anti-corrosion coatings. This device produces concentrations of chemically-active species, similar to those observed in low-pressure plasma deposition systems, with the advantage of operating in an ambient pressure atmosphere. This paper describes measurements of the properties of a bench-scale plasma jet operating in etch and deposition mode. The jet effluent was characterized by various methods, including optical emission spectroscopy. Films deposited on metallic and insulating substrates have been characterized by optical microscopy and surface analytical techniques. The potential for scale-up of this process to treatment of reactor components is discussed.

### **1. Introduction**

Plasma processing has found widespread application in materials processing, particularly in the fields of semiconductor manufacture [1] and in the production of tribological and optical coatings [2]. Plasmas can produce materials that are not otherwise obtainable, since the plasma environment alters the normal pathways that chemical systems take from one stable state to another. However, most plasma processes require reduced pressure to operate, with the attendant disadvantages of vacuum systems and sample introduction chambers. The size of object to be treated is limited by the size of the vacuum chamber, and it would be impossible to treat an object already installed in a large facility. To overcome this disadvantage, methods have been developed to generate plasma at atmospheric pressure: with corona discharges [3], dielectric barrier discharges [4] and plasma torches [5]. These devices have been used in niche applications, but generally do not have many of the attractive features of a low-pressure plasma system.

Recently, the atmospheric-pressure plasma jet has been developed by Selwyn at Los Alamos National Laboratory [6–8]. This device operates at ambient atmospheric pressure with some of the advantages of the low-pressure discharge, including low gas temperature and high concentrations of desirable species. APJeT Inc.<sup>1</sup> is now manufacturing these units to the Los Alamos design. An EDJ-100A etching/deposition unit was recently purchased by Chalk River Laboratories (CRL) to evaluate potential applications of this technology to the Generation IV program [9].

This report describes experiments carried out at CRL to characterize the plasma jet unit. Optical emission spectroscopy was used to determine the active species in the plasma-forming region of the plasma jet and in the effluent. The results of etch rate measurements and deposition

---

<sup>1</sup> APJeT, Inc. 3900 Paseo del Sol, Santa Fe, NM 87507, U.S.A.

experiments with organo-metallic precursors are described. We conclude with a discussion of scale-up of the equipment to treat large components.

## **2. Description**

The APJeT atmospheric-pressure plasma jet unit is shown in Figure 1. Helium carrier gas flows between coaxial electrodes at a rate of 25–50 standard litres per minute (SLPM). Active gases, such as O<sub>2</sub>, are entrained in the He carrier at approximately 1% by volume of helium flow. The central electrode is biased with 200–500 W of 13.56 MHz radio frequency (RF) power. A plasma discharge is established in the annular gap between the biased and grounded electrodes, forming chemically-active species such as atomic and metastable molecular oxygen. The ionized gas flows out the open end of the coaxial electrode assembly at a velocity of approximately 12 m/s and impinges on the workpiece positioned approximately 2–20 mm downstream. When operating in this mode, the plasma jet can etch or treat the surface of substrates placed in its path. For deposition, a precursor such as silane (SiH<sub>4</sub>) or an organometallic compound such as TEOS (tetraethoxysilane), is injected into an alumina precursor feed tube. The feed tube passes through the central electrode and projects into the nozzle. The precursor flow mixes with the ionized gas stream flowing out of the annular discharge region, creating chemically-active species.

## **3. Plasma jet operation and characterization**

The plasma jet unit is mounted inside a ventilated acrylic box. An XYZ stage permits positioning of diagnostics in the effluent. A temperature-controlled substrate holder can also be mounted on the stage.

Operation of the unit is straightforward. Cooling water is turned on to the plasma jet unit and process gas flows are set with mass flow controllers. RF power is applied at approximately 200 W. The plasma usually strikes immediately and the RF power can then be ramped up to an administrative limit of 400 W in a few seconds, with no tendency to arc. The reflected power is kept below 1–2 W by an automatic matching network, which adjusts the impedance of the transmission line to suit changes in plasma impedance following alterations to gas flow and RF power settings. A photograph of the plasma-forming region of an operating plasma jet is shown in Figure 2.

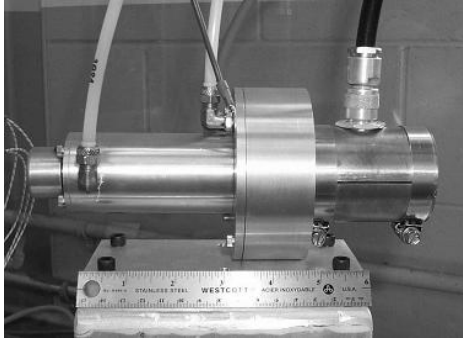


Figure 1 Plasma jet unit.

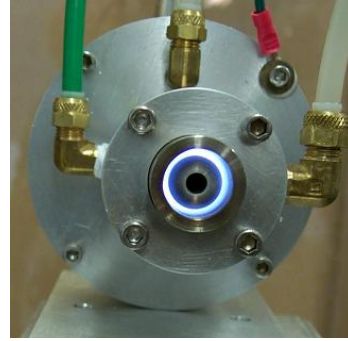


Figure 2 Operating plasma jet.

### 3.1 Temperature measurements

An advantage of the plasma jet is that the effluent is relatively cool, resulting in lower thermal stress to the part being treated. The variation in temperature with distance from the jet nozzle is shown in Figure 3. A Type K stainless steel sheathed thermocouple was scanned along the axis of the plasma jet while operating at 400 W RF power, 25 SLPM helium flow and 500 standard cubic centimetres per minute (SCCM) oxygen flow. The maximum temperature was 259°C at 2.5 mm from the end of the nozzle, which is “cold” when compared to the electron temperature necessary to cause ionization.

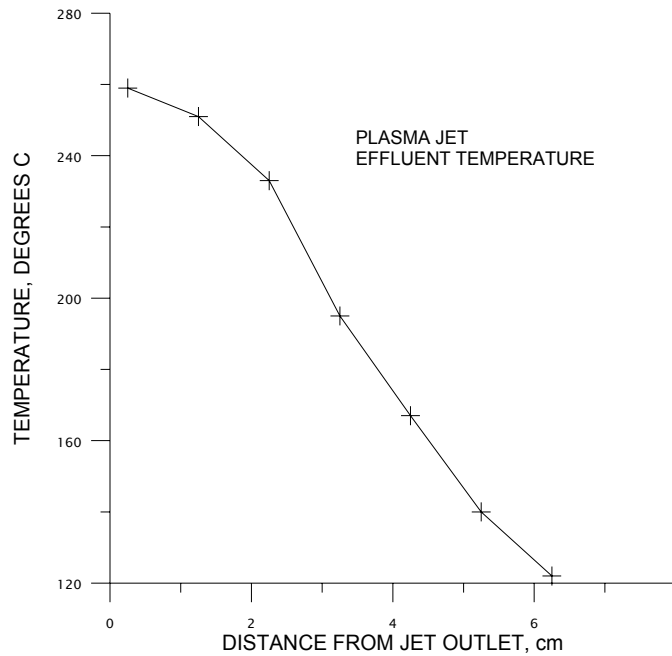


Figure 3 Temperature of plasma jet effluent, axial profile.

### 3.2 Spectroscopic characterization of the plasma jet

Optical emission spectroscopy provides information about the concentration of species created in the plasma-forming region between the electrodes, and about the species that survive in the effluent as they exit the nozzle. Spectra were acquired with a SPEX 1000m optical spectrometer over a range of 400 to 1000 nm, equipped with a SPEX Spectrum One liquid-nitrogen-cooled charge coupled device (CCD) detector. The plasma jet unit was operated at 400 W RF power, 25–50 SLPM He carrier flow and 500 SCCM O<sub>2</sub> flow for these measurements.

A spectrum measured with the light collection optics aligned along the cylindrical axis of the plasma jet (so that light was collected from the annular discharge region) is compared in Figure 4 to a spectrum where the collection optics were aligned orthogonal to the plasma-jet axis. The atomic lines in the spectrum looking along the cylindrical axis have peak heights about 500 times higher than those in the orthogonal-looking spectrum. Especially prominent are the atomic oxygen lines at 777 nm and 844 nm and the atomic helium lines at 588 nm, 706 nm and 668 nm. The wavelength and peak heights of the prominent lines and bands in the plasma jet spectra are listed in Table 1. Atomic lines are identified according to the National Institute of Standards and Technology (NIST) Atomic Spectra Database [10].

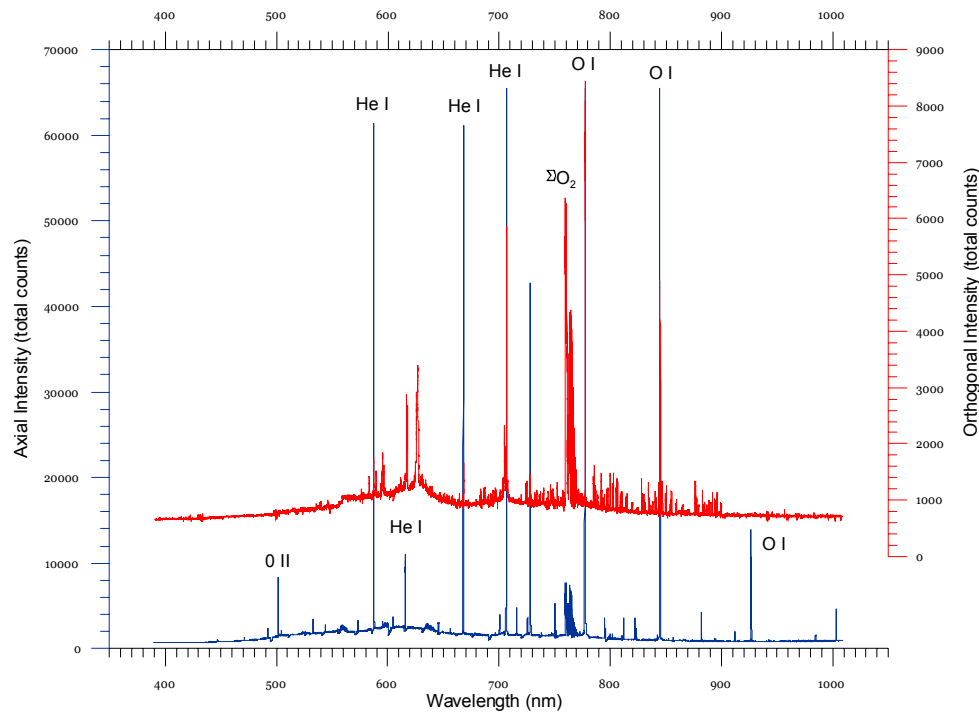


Figure 4 Optical emission spectra observed in the annular discharge region of the plasma jet (blue) and in the plasma jet effluent (red). The atomic lines from the plasma-forming region are approximately 500 times more intense than those in the spectrum taken from the effluent. Some prominent spectral lines are noted.

Orthogonal Spectrum		Axial Spectrum		Assignment
Wavelength (nm)	Peak Height (total counts)	Wavelength (nm)	Peak Height (total counts)	
		447.25	1076	He I
		501.65	8339	O II
		533.10	3493	O I
		543.65	2823	O I
587.46	1770	587.65	>60000	He I
		645.54	3161	O I
668.02	1662	667.91	>60000	He I
706.78	5878	706.64	>60000	He I
728.27	1463	728.22	42 938	He I
777.52	8444	777.43	>60000	O I
795.14	1104	794.86	3654	O I
		822.28	3564	O I
844.80	4901	844.74	>60000	O I
		926.70	14038	O I
$^1\Sigma O_2$ (758–770 nm)				

Table 1 Prominent emission lines detected in the plasma jet plasma-forming region (axial spectrum) and effluent (orthogonal spectrum). The detector saturates at 60000 counts.

As well as identifying the species present, other information about the plasma can be inferred from the spectroscopic data. The rotational temperature of the plasma in the annular discharge region was determined from the rotational fine structure of the (0, 0) transition of singlet sigma metastable molecular oxygen,  $^1\Sigma O_2$ . Several bands arising from  $^1\Sigma O_2$  were observed in the plasma jet spectrum. The strongest band was at 758–770 nm; spectra of this band measured axially and orthogonally are shown in Figure 5. The inferred rotational temperature is approximately 250°C. This result compares favourably with the translational temperature of 260°C previously measured by thermocouple, suggesting, as expected, a highly collisional plasma.

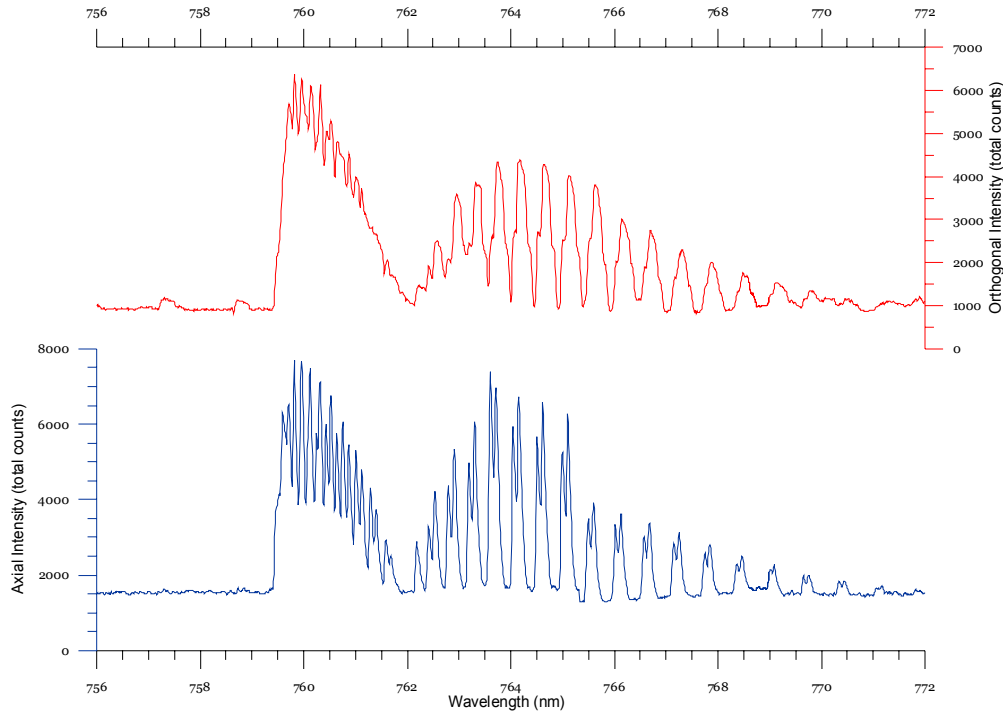


Figure 5 Axial (blue) and orthogonal (red) spectra of  $^1\Sigma O_2$ .

### 3.3 Distribution of species in the plasma jet effluent

The presence of chemically-active species in the plasma jet effluent is of importance to the application of the plasma jet. Information about the concentration of these species can be obtained spectroscopically, as described earlier, or by measurements of the physical effects, such as etch rate, on substrates placed in the effluent.

Figure 6 compares the etch rate of polyamide (Kapton<sup>®</sup>) film to the relative peak heights of  $^1\Sigma O_2$  (758–770 nm) and the  $3^5P-3^5S$  transition of atomic oxygen at 777 nm as a function of distance from the plasma jet outlet<sup>2</sup>. Peak heights and etch rates have been normalized to their values at the plasma jet outlet. A comparison of the trends of these particular atomic and molecular species concentrations (inferred from relative peak height of each species) suggests that atomic oxygen is likely the more important species for etching polyamide.

---

Kapton<sup>®</sup> is a registered trademark of Dupont.

<sup>2</sup> It is thought that the etching of polyamide and other polymers is due to the presence of atomic oxygen or excited molecular oxygen species.

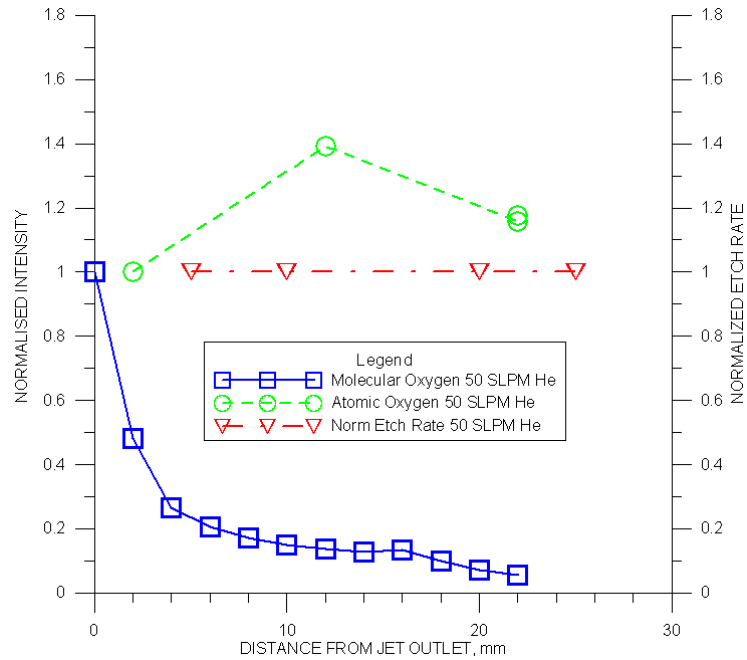


Figure 6 Normalized atomic and molecular oxygen peak heights and Kapton etch rate as a function of distance from the nozzle outlet.

#### 4. Deposition experiments

Thin films can be grown on substrates placed in the plasma jet effluent by injecting suitable precursor materials into a glass or alumina tube which passes through the hollow centre conductor of the plasma jet. The precursors exit the tube into the nozzle region where they interact with the ionized gas flowing out of the annular plasma-forming region to form active species that will grow oxide films on the substrate. This technique has already been used to grow micron-thick SiO<sub>2</sub> films on Si substrates [11].

Introducing appropriate precursors for thin-film growth into the low-temperature plasma jet presents a practical problem. Typical solid thin film materials, such as oxides of silicon or zirconium, have very high vaporization temperatures. Gaseous forms of most of these materials, for example, SiH<sub>4</sub> are often toxic or pyrophoric and are thus difficult to handle in a system open to ambient atmosphere. We have investigated the use of zirconium tetra-tert-butoxide (ZTB), a less toxic and reactive compound, as a precursor for zirconium oxide films, which could provide a corrosion and wear-resistant coating for in-core and out-core components. ZTB has been demonstrated as a precursor for ZrO<sub>2</sub> films in low-pressure plasma systems [12,13].

ZTB is liquid at room temperature, which allows vapour to be introduced into the plasma jet precursor feed tube by bubbling with an inert carrier gas such as He. However, ZTB is also extremely sensitive to moisture, rapidly hydrolyzing to a granular powder in the presence of trace amounts of water. Early attempts to use ZTB as a precursor for the plasma jet failed because of rapid clogging of the bubbler system. Careful purging of the gas lines, use of ultra-high purity

He as the carrier gas and additional drying of the carrier gas with Zeolite traps was found to be necessary to prevent clogging. A schematic of the present system for handling ZTB precursor is shown in Figure 7.

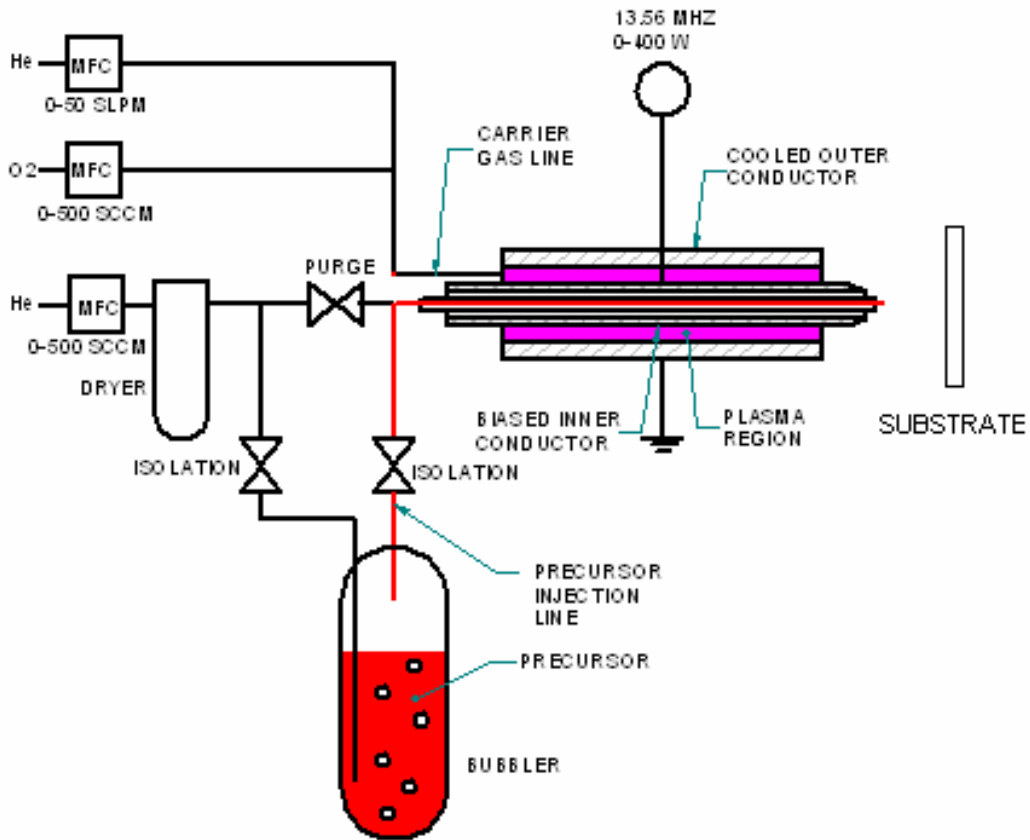


Figure 7 Schematic of plasma jet system set-up for ZTB precursor handling.

Before proceeding with deposition experiments, spectroscopic measurements of the effluent were made to confirm the presence of species from the dissociation of precursor molecules in the plasma. Figure 8 compares a spectrum obtained without bubbler flow (blue) to a spectrum obtained with helium flow through a ZTB-filled bubbler (red). A rotational band attributed to the vibrational-rotational band of C<sub>2</sub> at 512–520 nm is observed with bubbler flow on.

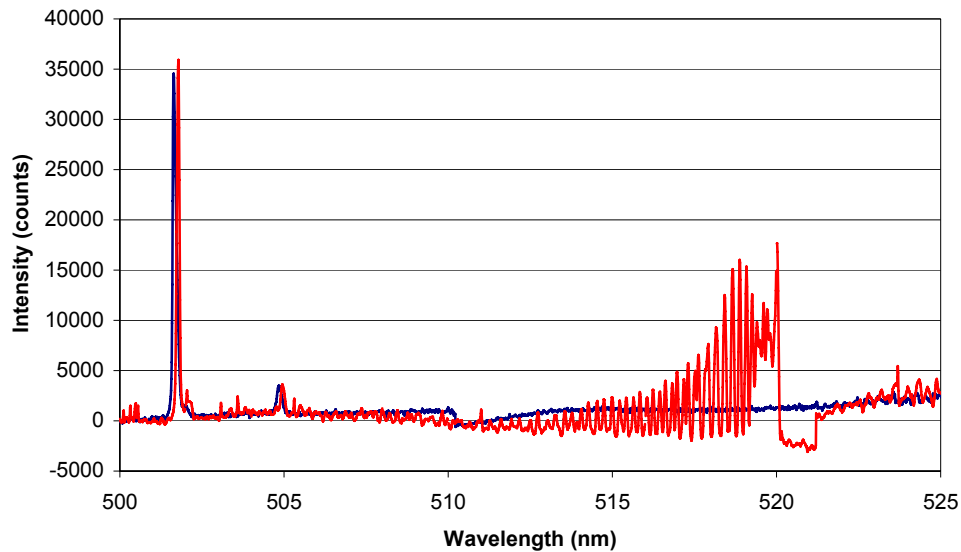


Figure 8 Orthogonal spectrum of plasma jet effluent with ZTB bubbler flow on (red) and off (blue).

Using the system shown in Figure 7, preliminary deposition experiments were carried out in the following manner. Substrates of silicon wafers, or Hastelloy<sup>®</sup> sheet, were cleaned in dilute HCl and de-ionized water, clamped in a temperature-controlled holder and masked to control the deposition area to a circle of 1 cm diameter. The holder was positioned about 5 mm from the plasma jet nozzle. The gas lines were purged with high-purity He and the substrate heated to the required temperature. A “cleaning cycle” was then started by operating the plasma jet on a He/O<sub>2</sub> feed for about 10 minutes at 400 W RF power, 50 SLPM He flow and 500 SCCM O<sub>2</sub> to etch residual contaminants from the surface of the substrate.

At the conclusion of the cleaning cycle, the bubbler isolation valves were opened and high-purity He flow to the bubbler was started while the discharge was maintained by the He/O<sub>2</sub> feed. A visible film was formed on silicon and Hastelloy<sup>®</sup> substrates after 2–30 minutes deposition time. The resulting films were classified as “thick” and “thin” by their visual appearance. Figure 9 shows a typical “thick” film grown on a silicon substrate. The view to the right is magnified 50x. The film presents a rough, scaly appearance and shows interference fringes when viewed in oblique light. Figure 10 shows a typical “thin” film grown on a silicon substrate. In this case, the film appears to be smoother and much thinner.

---

Hastelloy<sup>®</sup> is a registered trademark of Haynes International, Inc.

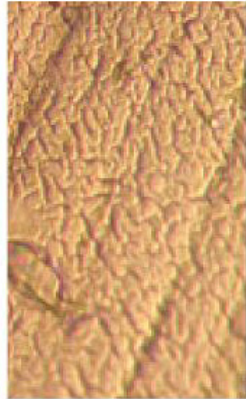


Figure 9 “Thick” film. View to the right is magnified 50x.



Figure 10 “Thin” film. View to the right is magnified 50x.

Table 2 summarizes the operating parameters that were varied during these tests and the resulting films.

“Thick” films	High bubbler flow rate (>250 sccm)
	Long deposition times (>15 minutes)
	Low substrate temperature (<250 °C)
“Thin films”	Low bubbler flow rate (<250 sccm)
	Short deposition times (<15 minutes)
	High substrate temperatures (>250 °C)

Table 2 Summary of results obtained by varying process parameters.

A Secondary Ion Mass Spectrometry (SIMS) depth profile (Figure 11) of a “thick” film on a silicon substrate was obtained with a Cameca IMS 6F instrument. Peaks of elemental zirconium, oxygen and zirconium oxide are clearly observed on the silicon substrate.

## 5. Process scale-up

The experiments described here are at a very preliminary stage, having demonstrated the deposition of zirconia-based thin films on metal and ceramic substrates in ambient atmosphere on a bench-scale and under laboratory conditions. It is important to note that the atmospheric-pressure plasma process has been scaled up for treatment of product on a large scale for other applications, providing confidence that the plasma jet can be adapted to coating processes suitable for use in the nuclear industry.

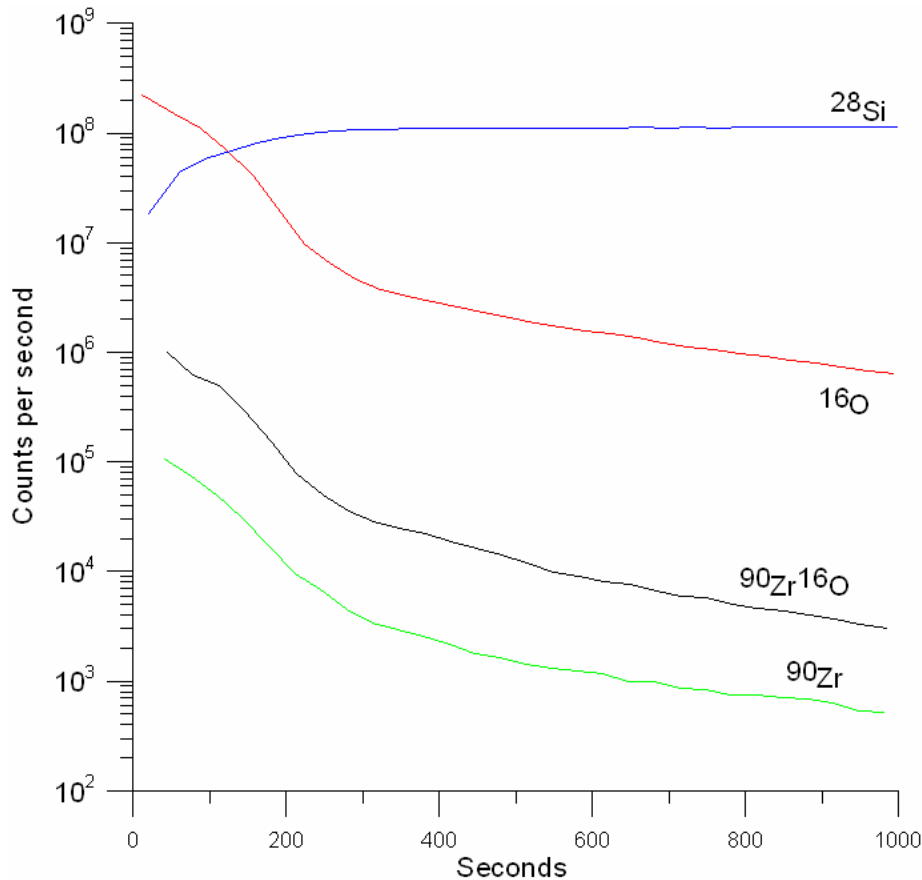


Figure 11 SIMS depth profile of “thick” film on silicon substrate.

For example, the plasma jet can be mechanically scanned over the area to be treated<sup>3</sup>, or the shape of the exit aperture can be altered to suit the product. APJeT have developed a linear plasma jet device for treating flat sheets of material. The substrate material is rolled in strip form under a linear slot aperture for treatment. The device can be manufactured to essentially any width to suit the product. APJeT have also developed a custom machine for the treatment of very large areas of fabric at rates of up to 120 ft/min. The unit contains eight 10-KW linear plasma jet units. Fabric to be treated is fed from a roller, passes vertically through the machine and is taken up on a second roller.

One major problem with scale-up of this technology is the very high flow rates of helium that are required to prevent arcing between the electrodes and to transport active species to the substrate before the active species decay. The bench-scale unit described earlier requires helium flow rates of 25–50 SLPM to treat a few cm<sup>2</sup> and will exhaust a standard helium cylinder in a few hours of operation. One technique to reduce helium consumption is to capture and recycle the helium cover gas, which takes little part in the ionization process, except to prevent arcing between the electrodes. This technique is utilized in the pilot-scale APJeT unit described above. Another possibility is to operate the plasma jet with less-expensive carrier gas. A group at the

<sup>3</sup> Surfex Technologies LLC, 3617 Hayden Avenue, Culver City, CA 90232.

University of Essen has reported operation of an APJeT plasma jet unit on Ar/O<sub>2</sub> and He/O<sub>2</sub> mixtures [14].

## 6. Acknowledgements

The authors thank Sumi Wren<sup>4</sup> for many of the spectroscopic measurements and the calculation of the rotational temperature reported in Section 3, Andrew Than Do for the SIMS analysis and Glenn McRae for enlightening discussions.

## 7. References

- [1] Schmid H., Kegel B., Petasch W., Liebel G., "Low pressure plasma processing in microelectronics", *Proceedings of the Joint 24<sup>th</sup> International Conference on Microelectronics (MIEL) and 32<sup>nd</sup> Symposium on Devices and Materials SD '96*, Nova Gorica, Slovenia, 1998, pp.17-35.
- [2] Pauleau Y., "Materials and processes for surface and interface engineering", *Proceedings of ASI*, Bonas, France, ISBN 0-7923-3458-2, 1994.
- [3] Goldman M., Goldman N., "Corona discharges", *Gaseous Electronics*, Vol. 1, Hirsch M.N., Oskam H.J., Eds., New York Academic, 1978, pp. 219-290.
- [4] Eliasson B., Kogelschatz U., "Non-equilibrium volume plasma chemical processing", *IEEE Transactions on Plasma Science*, Vol, 19, 1991 December, pp. 1063-1077.
- [5] MacRae D.R., "Plasma arc process systems, reactors, and applications", *Plasma Chemistry Plasma Processing*, Vol. 9, Number 1, 1989, pp. 858-1185.
- [6] Jeong J.Y., Babayan S.E., Schütze A., Tu V.J., Park I., Henins I., Selwyn G., Hick R.F., "Etching polyamide with a non-equilibrium atmospheric-pressure plasma jet", *Journal of Vacuum Science and Technology A*, Vol. 17, Number 5, 1999 September/October.
- [7] Selwyn G., Hicks R., "Atmospheric pressure plasma cleaning of contaminated surfaces", Los Alamos National Laboratory Report Number LA-UR-00-0631, 1999.
- [8] Babayan S., Selwyn G., Hicks R., (The Regents of the University of California, assignee), "Deposition of coatings using an atmospheric plasma jet", U.S. Patent 6,194,036 B1, February 27, 2001.
- [9] U.S. DOE Nuclear Energy Research Advisory Committee and Gen IV International Forum (GIF), "A technology roadmap for Generation IV nuclear energy systems" GIF002-00, December 2002.
- [10] Martin W.C., Wise W.C., "Atomic Spectroscopy", National Institute of Standards and Technology. <http://physics.nist.gov/Pubs/AtSpec/index.html>.
- [11] Babayan S.E., Jeong J.Y., Tu V.J., Park J., Selwyn G.S., Hicks, R.F., "Deposition of silicon dioxide films with an atmospheric-pressure plasma jet", *Plasma Sources Science and Technology*, Vol. 7, 1998, pp. 286-288.
- [12] Cho B-O., Wang J., Chang J.P., "Metalorganic precursor decomposition and oxidation mechanisms in plasma-enhanced ZrO<sub>2</sub> deposition", *Journal of Applied Physics*, Vol. 92, Number 8, 15b October 2002.

---

<sup>4</sup> Deep River Science Academy, Box 600, Deep River, ON K0J 1P0.

- [13] Cho B-O., Lao S., Sha L., Chang J.P., “Spectroscopic study of plasma using zirconium tetra-tert-butoxide for the plasma enhanced chemical vapor deposition of zirconium oxide”, *Journal of Vacuum Science and Technology A*, Vol. 19, Number 6, Nov/Dec 2001.
- [14] Niemi K., Wang, S., Schulz-von der Gathen V., Dobele H.F., “Discharge comparison of nonequilibrium atmospheric pressure Ar/O<sub>2</sub> and He/O<sub>2</sub> plasma jets“, *Applied Physics Letters*, 83, 2003, pp. 3272-3274.